Available online at www.sciencedirect.com
ScienceDirect
Trans. Nonferrous Met. Soc. China 29(2019) 178−185
Transactions of Nonferrous Metals Society of China
www.tnmsc.cn

Mechanism and application on sulphidizing flotation of copper oxide with combined collectors

Wan-zhong YIN[1,2], Qian-yu SUN[1] , Dong LI[1], Yuan TANG[1], Ya-feng FU[1], Jin YAO[1]

1. College of Resources and Civil Engineering, Northeastern University, Shenyang 110819, China;
2. College of Zijin Mining, Fuzhou University, Fuzhou 350116, China

Received 3 January 2018; accepted 2 July 2018

Abstract: The effect of sodium butyl xanthate (NaBX) and dodecylamine (DDA) as combined collector on the sulphidizing flotation of copper oxide was investigated by flotation test, fluorescent pyrene probe, zeta potential, and infrared spectroscopy analyses. The micro-flotation results show that combined use of NaBX+DDA yields better effect than using NaBX at pH 7−11 only, and the optimal molar ratio of NaBX to DDA is 2: 1. The actual ores flotation shows that when the dosage of NaBX+DDA is (100+54) g/t, the copper concentrate grade and recovery are 15.93% and 76.73%, respectively. The fluorescent pyrene probe test demonstrates that the NaBX+DDA can reduce the micelle concentration in the pulp. The zeta potential and the infrared spectroscopy analyses indicate that chemical adsorption, hydrogen-bonding and electrostatic interaction can help to adsorb NaBX+DDA on the surface of malachite. Meantime, copper xanthate and copper-amine complexes may be generated during the adsorption process.
Key words: copper oxide; combined collector; flotation; adsorption; infrared spectroscopy

1 Introduction

Copper is an indispensable industrial material and a vital strategic resource for the development of national economy, national lives, and defense-related science [1]. Although most of the copper metal is extracted from copper sulfide minerals, the exploitation of copper oxide has been gradually increasing for years due to the reduction of copper sulfide resources [2−4]. Chemical methods and flotation are usually exclusively used for separation of copper oxide. However, chemical methods of acid leaching, ammonia leaching, bacterial leaching, etc, are plagued with various problems from poor performance for diverse properties ores, long production cycle tremendous consumption of regents, to inherent corrosion for equipment [5,6]. Therefore, the application of flotation in copper oxide ore has attracted extensive attention [7−9].

The flotation of copper oxide can be mainly divided into direct flotation and sulphidizing flotation. The collectors for direct flotation are fatty acids, fatty amine, petroleum sulfonate and hydroximic acids [10,11]. Recently, LI et al [12] synthesized α-hydroxyoctyl phosphinic acid as a powerful collector and achieved good result for direct flotation. FUERSTENAU et al [13] evaluated the absorption property and flotation effect of chelating collectors on various copper oxide ores. KIM et al [14] found that *Rhodococcusopacus* bacteremia can be used as biological collector due to its adsorption ability on the malachite surface during different growing periods. Although the above study is valuable, the commercial application of direct flotation is restrained due to inferior selectivity of gangue minerals, high cost of chemical reagents and low grade of concentrates [15]. The sulphidizing flotation, which is realized by adding sulfurizing agents during flotation, can change the surface structure of copper oxide, making its properties similar to that of copper sulphide surface [16]. So far, sulphidizing flotation has become the most widely-used industrial approach for the utilization of copper oxide ores. If xanthate collector is used solely in complex copper oxide ores, its collection capability is limited. However, excessive amount of sulfurizing agents have great adverse effects on the flotation of copper oxide [3].

The combined anionic/cationic collectors have been

Foundation item: Projects (51504053, 51374079) supported by the National Natural Science Foundation of China
Corresponding author: Qian-yu SUN; Tel: +86-15841813136; E-mail: sunnyway1213@126.com
DOI: 10.1016/S1003-6326(18)64926-X

widely used in the flotation of some oxidized ores, which plays a synergistic effect in enhancing the hydrophobicity of the mineral surface [17,18]. The synergistic effects can attribute to that when the mineral surface is negatively charged, the cation is adsorbed on the mineral surface preferentially, and then the anion is electrically neutralized to generate co-adsorption, enhancing the floatability of minerals by complex effects [19,20]. In particular, MEHDILO et al [21] found that the combined collectors of anionic and cationic had stronger adaptability in the pulp, which reduced the consumption of the sulfurizing agent and improved flotation index. So far, researches about the combined collector for copper oxide ores have been mainly based on two kinds of anionic collectors, namely hydroxamate and xanthate [22,23]. However, studies about the anion and cation collectors used as combined collectors for sulphidizing flotation of copper oxide minerals were scarce.

In this work, an innovative use of NaBX+DDA as combined collector for copper oxide flotation is proposed. The flotation performance of malachite was evaluated under different conditions such as dosages of collectors, pH values, and reagent ratios. The evaluation experiment was then validated by actual ore flotation. At last, the synergistic mechanism of NaBX+DDA was investigated by fluorescent pyrene probe, zeta potential, and infrared spectroscopy analyses.

2 Experimental

2.1 Materials and reagents

The raw ore was obtained from the Tonglushan, Hubei Province, China. The 37−74 μm product of malachite was obtained from raw ore by manual selection, crushing, grinding, screening and repeated table-concentrator. The purity of malachite was 95% by chemical analysis, and the X-ray diffraction (XRD) pattern is shown in Fig. 1(a). The XRD pattern of raw ore (Fig. 1(b)) shows that the main copper minerals include malachite, covellite, pseudo malachite and azurite. The X-ray fluorescence analysis and chemical phase analysis of Cu are shown in Tables 1 and 2, respectively. The raw ore contained 1.25% Cu and 61% copper oxide, while metals such as gold, silver and iron were also found. In addition, S and P contents were not high and gangue composition was mainly SiO_2.

Sodium butyl xanthate (NaBX) and dodecylamine (DDA) were used as the flotation collectors, sodium sulfide as the sulfurizing agent, and sodium silicate as the inhibitor. Hydrochloric acid and sodium carbonate were used for pH regulator in flotation and zeta potential measurement. The $2^{\#}$ oil was used as frother. Deionized water was used in the preparation of solutions for all experiments.

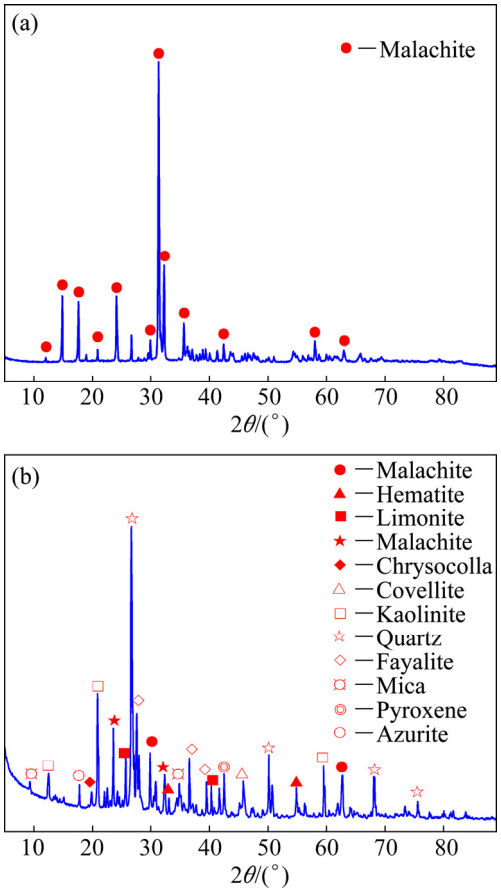

Fig. 1 XRD patterns of malachite sample (a) and raw ore sample (b)

Table 1 Multi-elemental analysis of raw ore (mass fraction, %)

Cu	Fe	CaO	MgO	SiO_2
1.25	30.3	4.09	0.89	35.21
S	P	w(Au)/(g·t^{-1})	w(Ag)/(g·t^{-1})	
3.12	0.07	0.81	6.7	

Table 2 Phase analysis of copper

Phase	Content/%	Distribution/%
Primary copper sulphide	0.20	16.29
Secondary copper sulphide	0.29	23.01
Free copper oxide	0.62	49.83
Combined copper oxide	0.14	10.87
Total copper	1.25	100.00

2.2 Flotation testing

The micro-flotation was carried out in the 40 mL XFGC-II flotation machine with an axial rotation speed of 1600 r/min. For each test, 5 g malachite was separately conditioned with Na_2S, NaBX/NaBX+DDA and $2^{\#}$ oil at desired pH value for 3 min (the NaBX+DDA were separately conditioned for 1.5 min), and then kept collecting the flotation froth for 5 min,

dried and weighed up the froth concentrate to calculate the recovery. Each flotation condition was repeated three times and then drew an error bar diagram.

The procedure of actual ore flotation was prepared as follows: Firstly, 600 g raw ore sample and 0.5 g sodium carbonate were added into the ball mill to obtain about 80% passing of 74 μm, which was then put into XFDIII−1.5 L flotation machine for selective flotation of sulphide minerals. The flotation tailing was diluted to 3.5% and then desliming treatment was conducted in the XCS-Φ25-type cyclone at a feed pressure of 0.25 MPa. Secondly, a certain amount of silicon-containing inorganic salts and sodium carbonate were added to the desliming sample that was stirred for 10 min. Then, the desliming sample was placed into XFDIII−1 L flotation machine. Afterwards, the Na_2S, NaBX and $2^{\#}$ oil were separately conditioned for 3 min (the NaBX+DDA were separately conditioned for 1.5 min). Thirdly, the collection of froth was conducted for 5 min. Then, the open-circuit test was carried out five times according to the process flow. At last, the flotation concentrates and tailings were dried and weighed, and the content of Cu was analyzed as well.

2.3 Zeta potential measurements

Malvern Instruments Nano-ZS90 zeta potential was used to measure the change of potential before and after malachite treatment. The malachite sample was ground in an agate mortar till the particles were smaller than 5 μm, which was then mixed with 100 mL water to form suspension liquid. Then, pH regulators, sulfidizing reagent and collectors were added into pulp. Subsequently, the suspension liquid was magnetically stirred for 10 min before being settled for 10 min. Lastly, the supernatant was extracted for measurement.

2.4 Fluorescent pyrene probe

The 2 g malachite with grain size of 37−74 μm, 0.1 mL pyrene ethanol solution and a certain amount of collectors were added into the 50 mL flask. The mixture was diluted to the prescribed volume and vibrated in the thermostatic oscillator for 24 h. Subsequently, the suspension was kept standing for 3 h, and then the supernatant was extracted for pyrene analysis by fluorescence spectrophotometer. The pyrene has five electron vibrating peaks, with corresponding emission intensity from I_1 to I_5. I_3/I_1 was defined as the index for the micropolarity of the environment. In the initial setting, the excitation wavelength of fluorescence scanning was 335 nm, the excitation slit was set to be 10 nm, and the emission slit was set to be 4 nm.

2.5 Infrared spectroscopy

Infrared spectroscopy was used to study the mechanism of interaction between mineral and regent. The malachite was ground to −5 μm by agate mortar. Then, samples were added to 35 mL aqueous solution without and with regents. After being stirred for 20 min, the samples were washed three times by deionized water. Subsequently, the obtained samples were dried at 40 °C and made with a KBr pellet for the infrared spectroscopy measured at 4000−400 cm^{-1}.

3 Results and discussions

3.1 Micro-flotation

The influence of NaBX concentration on micro-flotation with single collector and combined collector is shown in Fig. 2. It is found that when the concentration of Na_2S is 4×10^{-4} mol/L, the combined collector (NaBX+DDA) yields a better flotation recovery than single NaBX collector as NaBX concentration increases during the sulphidizing flotation. When Na_2S is at a lower concentration, the NaBX+DDA combined collector outmatches the single NaBX in malachite recovery as soon as the concentration exceeds 2×10^{-4} mol/L. The flotation results suggest that the NaBX+DDA combined collector has a stronger collecting effect than single NaBX during sulphidizing flotation.

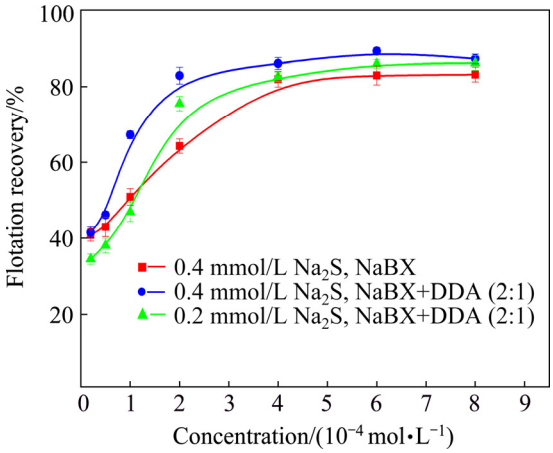

Fig. 2 Effect of NaBX concentration on micro-flotation recovery with different collectors at pH 7

The mineral flotation performance can be optimized by adjusting appropriate proportion of different collectors [24]. The results of flotation tests with different molar ratios of NaBX to DDA are shown in Fig. 3. When the molar ratio of NaBX to DDA is 5:1, the recovery is slightly lower than that when NaBX is alone used. However, when the proportion of DDA in NaBX+DDA is gradually increased, the flotation recovery enhances accordingly. Thus, it is determined that flotation recovery reaches the highest value when the molar ratio of NaBX to DDA is 2:1.

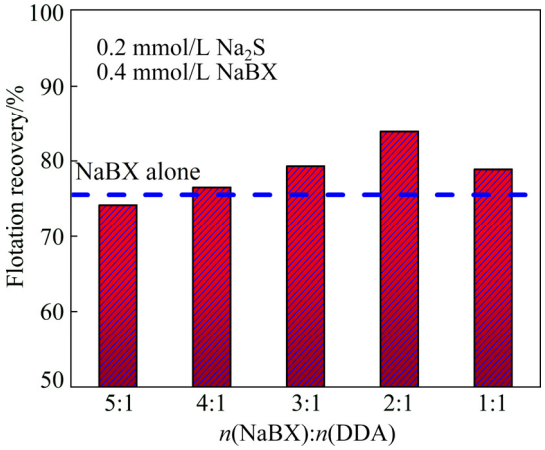

Fig. 3 Effect of collectors with different molar ratios on flotation recovery at pH 10

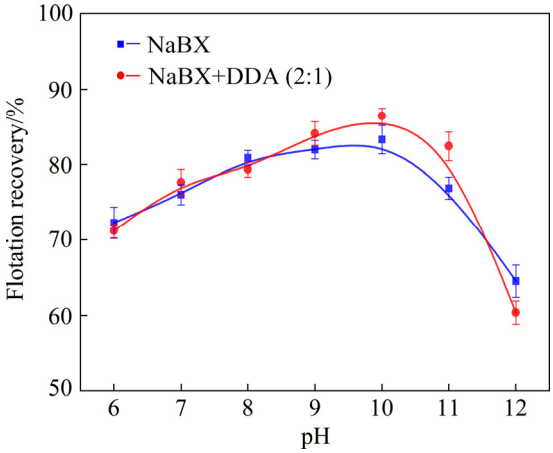

Fig. 4 Effect of pH value on sulphidizing flotation recovery with different collectors

Figure 4 shows the sulphidizing flotation effect of NaBX+DDA and NaBX on malachite at different pH values. When the pH ranges from 7 to 11, the flotation effect of NaBX+DDA is significantly better than that of single NaBX. Particularly, when pH is at 10, the recovery reaches the peak of about 86.5%.

3.2 Actual ore flotation

The raw ore sample was prone to sliming and contained some copper sulfide. Pre-flotation of sulfide minerals and de-sliming were proceeded prior to copper oxide flotation. Since this work was primarily focused on the performance of NaBX+DDA as combined collector in copper oxide flotation, the flotation of copper sulfide concentrates and fine ore slime was not described in detail. However, the workflow of copper oxide flotation is demonstrated in the dashed box in Fig. 5, while the reagent system and product index are shown in Table 3.

Under the condition that the dosage of Na_2S used for roughing copper oxide is 2000 g/t, when NaBX+

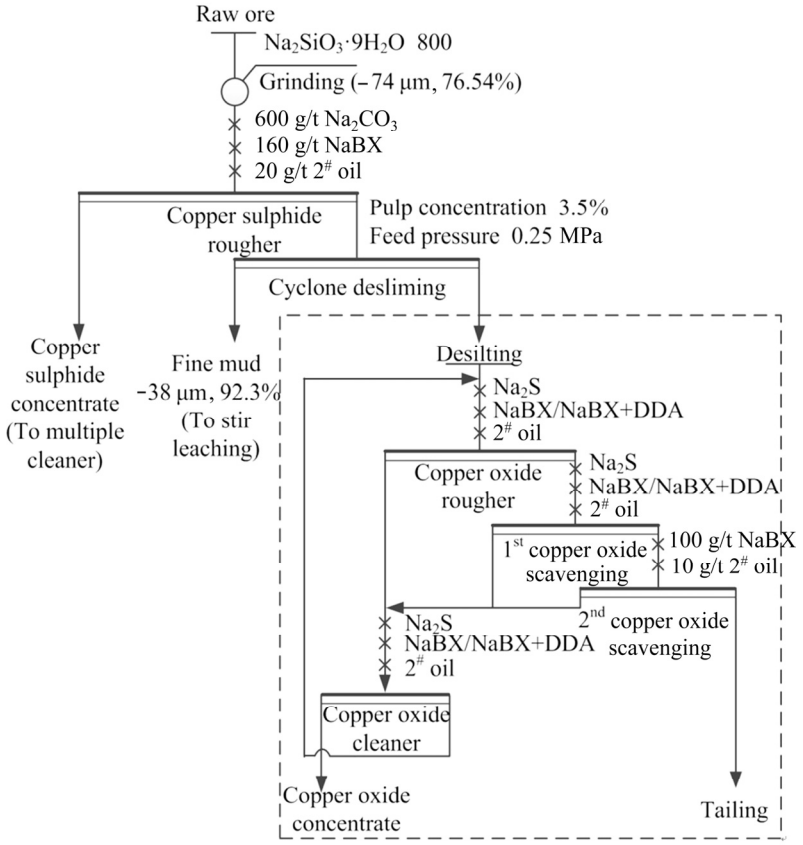

Fig. 5 Mineral separation workflow of raw ore

Table 3 Reagent system and flotation index of copper oxide flotation

Copper oxide roughing reagent system	Product name	Yield/%	Grade/%	Recovery/%	Relative recovery/%
	Raw ore	100.00	1.25	100.00	−
	Treated ore	17.89	0.88	57.61	100.00
2000 g/t Na_2S; 100 g/t NaBX; 20 g/t $2^{\#}$ oil	Concentrate	3.22	16.21	41.76	72.51
	Tailing	78.89	0.25	15.84	27.49
2000 g/t Na_2S; (100+54) g/t NaBX+DDA; 20 g/t $2^{\#}$ oil	Concentrate	3.47	15.93	44.21	76.73
	Tailing	78.64	0.21	13.39	23.27
2000 g/t Na_2S; 200 g/t NaBX; 20 g/t $2^{\#}$ oil	Concentrate	3.41	15.52	43.04	74.72
	Tailing	78.70	0.23	14.56	25.28
3000 g/t Na_2S; 100 g/t NaBX; 20 g/t $2^{\#}$ oil	Concentrate	3.01	16.59	39.89	69.25
	Tailing	79.10	0.28	17.71	30.75

*The dosage of reagent in cleaning and primary scavenging was 1/4 and 1/2 of those in roughing, respectively.

DDA is used as combined collector, the relative recovery of copper concentrate is 76.73%, which is higher than the relative recovery of 72.51% when the NaBX is used alone. In addition, their concentrate grades are at the same level. When NaBX is used alone, though proper increased dosage of NaBX or Na_2S can lead to a minor improvement in copper recovery and grade, the overall index is still inferior to that achieved by NaBX+DDA. The flotation result of actual ore proves that the NaBX+DDA truly has good effects on the sulphidizing flotation of copper oxide.

3.3 Micropolarity of malachite surfaces

The micelle concentration formed by collectors in the malachite particle suspension was determined by measuring the micro-polarity of pyrene. In aqueous solution, the I_3/I_1 ratio was 0.5:1−0.6:1; in micelle solution, the ratio was 0.8:1−0.9:1; while in nonpolar solutions, it exceeded 1:1 [25]. As shown in Fig. 6, it can be seen that as the concentration increases, the micropolarity (I_3/I_1) in NaBX and DDA solutions is enhanced slowly, and the generated micelle concentrations are about 3×10^{-4} mol/L and 2×10^{-4} mol/L, respectively. When NaBX and DDA are added at the same time, the generated micelle concentration is about 0.8×10^{-4} mol/L, which is lower than that when either NaBX or DDA is used. This may be resulted from the fact that DDA cations intercalate between the xanthate anions. Under that condition, negative and positive ions are neutralized, thus reducing the electrostatic repulsion between molecules [21]. The combined use of NaBX+DDA can contribute to the formation of micelles on the malachite surface, resulting in the improvement of flotation recovery.

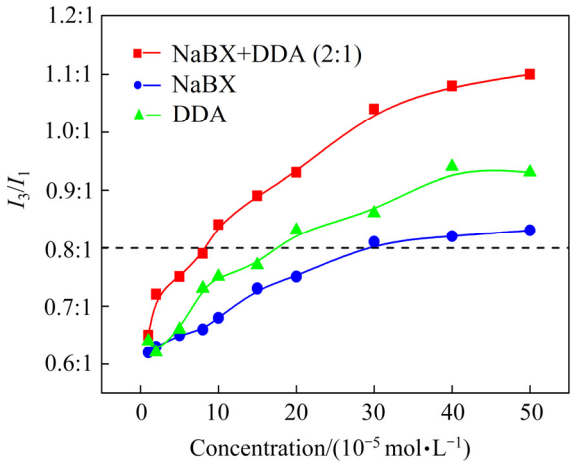

Fig. 6 Relationship between I_3/I_1 in malachite suspensions and concentration of different collectors

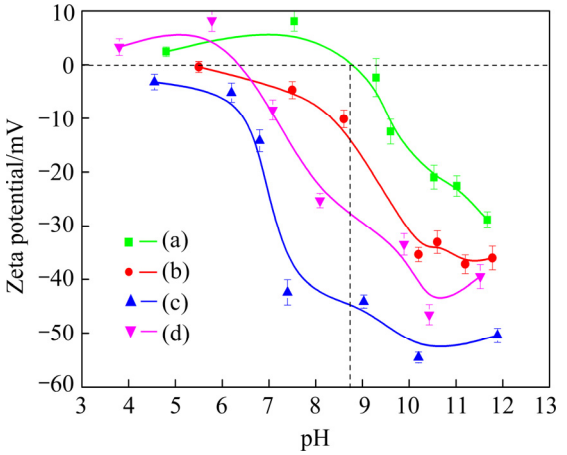

Fig. 7 Zeta potential of malachite (a), malachite+Na_2S (b), malachite+Na_2S +NaBX (c) and malachite+Na_2S+NaBX+DDA (d) as function of pH

3.4 Zeta potential

Figure 7 shows the zeta potentials of malachite as a function of pH without or with reagents. It can be found that the isoelectric point of malachite is about 8.8. When Na_2S is added, the curve of malachite surface charge moves towards the negative direction. This is due to the fact that HS^- and S^{2-} ions released by hydrolyzed Na_2S adhere to metal ions or metal hydroxyl complexes on the

malachite surface, and the resultant copper sulfide leads to increased negative charges on the mineral surface [26]. When NaBX is added, the negatively charged malachite surface moves to more negative charges, which suggests the occurrence of chemical adsorption of NaBX on the sulfide malachite surface. After the addition of DDA, the surface potential moves towards the positive direction. This implies that the cationic collector DDA ionizes RNH_4^+, and then it is adsorbed on the negatively charged mineral surface through electrostatic adsorption. In addition, it should be noted that when the electrical properties of malachite surface changes positively at the pH value less than 6, the surface potential exceeds the original potential of malachite, which indicates that hydrogen bonds might exist on the mineral surface [27].

3.5 Infrared spectrum

Figure 8(a) shows the infrared spectrum of NaBX. The peak at 3405 cm^{-1} is the stretching vibration of —OH, which is possibly due to the fact that NaBX powders absorbed water from the air. However, the peaks at 2961, 2867, and 1400 cm^{-1} are the asymmetric, symmetric stretching vibration and bending vibration of $—CH_3$, respectively; those at 2925 and 1460 cm^{-1} are the asymmetric, stretching and bending vibration of $—CH_2^-$; those at 1175 and 1105 cm^{-1} are the stretching vibration of C—O—C; those at 1265 and 1030.6 cm^{-1} are the stretching vibration of C═S; the peak at 686 cm^{-1} is the stretching vibration of C—S. Figure 8(b) shows the infrared spectrum of DDA. The stretching vibration peaks of $—NH_2$ are at 3334 cm^{-1} and 3122 cm^{-1}, respectively; the asymmetric and symmetric stretching vibration peaks of $—CH_3$ are at 2960 cm^{-1} and 2851 cm^{-1}. The bending vibration peak of $—CH_3$ is at 1400 cm^{-1}. The asymmetric stretching vibration peak of $—CH_2—$ was at 2920 cm^{-1}; the adsorption peak of $—NH_3^+$ at 2158 cm^{-1} is the combined tone of symmetric and asymmetric vibration, while the asymmetric bending vibration peaks are at 1580 cm^{-1} and 1487 cm^{-1}. Lastly, the stretching vibration peak of C—N is at 1142 cm^{-1}.

Figure 9(a) shows the infrared spectrum of malachite. The stretching vibration peaks of —OH are located at 3405 cm^{-1} and 3315.2 cm^{-1}. The asymmetric stretching vibration peaks of CO_3^{2-} are at 875 cm^{-1} and 743 cm^{-1}, while the symmetric stretching vibration peaks are at 1097.1 cm^{-1} and 818 cm^{-1}. Lastly, the bending vibration peaks are at 875 cm^{-1} and 743 cm^{-1}. Owing to the complex structure of malachite, Cu—(O, OH) presents two different coordination polyhedrons, with the stretching vibration peak of Cu—O at 570 cm^{-1} and that of Cu—OH at 528 cm^{-1} and 485 cm^{-1}. The infrared spectrum of the sulfurized malachite is illustrated in Fig. 9(b). It is found that the stretching vibration peak of —OH shifts from 3315 cm^{-1} to 3304 cm^{-1}, while the bending vibration peak is weakened and shifts from 1047 cm^{-1} to 1044 cm^{-1}. Moreover, the stretching vibration peak of Cu—OH disappears at 485 cm^{-1}, and a new lattice vibration peak of Cu—S appears at 431 cm^{-1}. This means that hydroxyl has reduced on the surface of malachite after sulfurization, and new copper sulfide substances are generated. The infrared spectrum of sulfurized malachite with NaBX is shown in Fig. 9(c). It is found that new characteristic peaks at 2960, 2925 and 2865 cm^{-1} can be attributed to the stretching vibration of $—CH_3$ and bending vibration of $—CH_2—$ in xanthate, which is in consistent with what Fig. 8(a) demonstrates. The peaks at 1251 and 1166 cm^{-1} are attributed to stretching vibration of C═S and C—O—C of xanthate and the low frequency offsets shifts by 13 cm^{-1} and 11 cm^{-1}. This shows that xanthate ions react with copper ions on the mineral surface and form metal xanthate by chemical adsorption [28]. Figure 9(d) shows the infrared spectrum of sulfurized malachite with NaBX+DDA. Compared with Fig. 9(c), the peak at 3120 cm^{-1} is attributed to the stretching vibration peak of

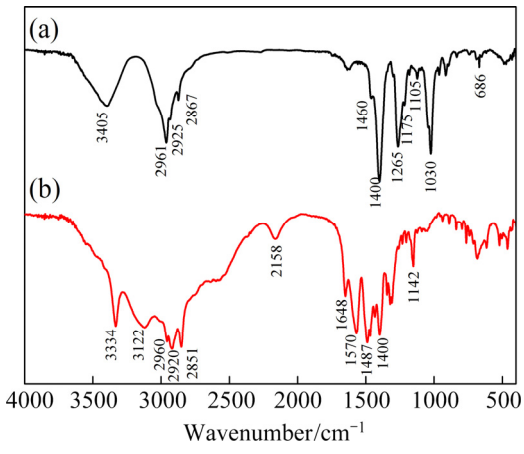

Fig. 8 Infrared spectra of NaBX (a) and DDA(b)

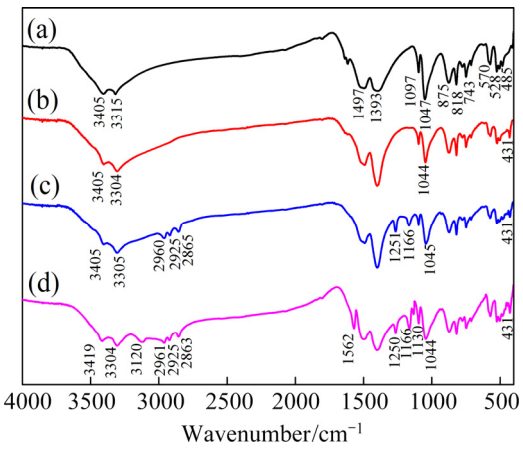

Fig. 9 Infrared spectra for malachite (a), malachite+Na_2S (b), malachite+Na_2S+NaBX (c), and malachite+Na_2S+NaBX+DDA (d)

—NH_2 in DDA as shown in Fig. 8(b). Two characteristic peaks at 1130 and 1562 cm^{-1} are attributed to the bending vibration peak of —NH_3^+ in DDA and the stretching vibration peak of the C—N, which shift by 12 cm^{-1} and 8 cm^{-1} to the low frequency, respectively. The shift may be resulted from the fact that a pair of lone pair electrons provided by the N ion of DDA chemically reacted with copper on the mineral surface and produced copper-amine complex [29]. In addition, the stretching vibration peak of —OH shifts from 3405 to 3419 cm^{-1}, which might be caused by the hydrogen bonding formed between the N atom and —OH on the malachite surface [30].

According to the results of infrared spectra (Fig. 9) and zeta potential (Fig. 7) analyses, the conclusion is that the NaBX+DDA is adsorbed on the surface of sulfurization through chemisorption, hydrogen-bonding adsorption, and electrostatic adherence, while the surface products are copper xanthate and copper-amine complex.

4 Conclusions

(1) The micro-flotation tests indicate that there is a synergistic effect of NaBX+DDA in sulphidizing flotation of malachite, and the optimal mole ratio of NaBX to DDA is 2:1 according to the test. When the pH value is within the range of 7−11, the combined use of NaBX+DDA yields a better recovery than NaBX used alone. In particular, when the pH value is 10, the recovery rate reaches its maximum.

(2) The flotation result of raw ores from Tonglushan mine is consistent with the micro-flotation. When the dosage of NaBX+DDA is (100+54) g/t, through the flow of single roughing, double scavenging, and single cleaning, the copper concentrate grade and recovery are 15.93% and 76.73%, respectively.

(3) The results of pyrene probe, zeta-potential and infrared spectrum measurement show that the NaBX+DDA can form micelles in pulp with lower dosage. Then, they are adsorbed on the surface of malachite in the form of chemical adsorption, hydrogen bonding and electrostatic adsorption, and produce copper xanthate and copper amine complex to enhance the flotation of minerals.

References

[1] LANZ B, RUTHERFORD T F, TILTON J E. Subglobal climate agreements and energy-intensive activities: An evaluation of carbon leakage in the copper industry [J]. World Economy, 2013, 36: 254−279.

[2] MA Yi-wen, HAN Yue-xin, ZHU Yi-ming, LI Yan-jun, LIU Hao. Flotation behaviors and mechanisms of chalcopyrite and galena after cyanide treatment [J]. Transactions of Nonferrous Metals Society of China, 2016, 26: 3245−3252.

[3] HUA Xiao-ming, ZHENG yong-fei, XU Qian, LU Xiong-gang. Interfacial reactions of chalcopyrite in ammonia-ammonium chloride solution [J]. Transactions of Nonferrous Metals Society of China, 2018, 28: 556−566.

[4] HAN Jun-wei, XIAO Jun, QIN Wen-qing. Copper recovery from Yulong complex copper oxide ore by flotation and magnetic separation [J]. JOM, 2017, 69(9): 1563−1569.

[5] KORDOSKY G A. Copper recovery using leach/solvent extraction/electrowinning technology: Forty years of innovation, 2.2 million tonnes of copper annually [J]. Journal of South African Institute of Mining and Metallurgy, 2002, 102(8): 445−450.

[6] BARTOS P J. SX-EW copper and the technology cycle [J]. Resources Policy, 2002, 28: 85−94.

[7] SOKIC M D, MILOSEVIC V D, STANKOVIC V D. Acid leaching of oxide-sulfide copper ore prior the flotation—A way for an increased metal recovery [J]. Hemijska Industrija, 2015, 69(5): 453−458.

[8] HOPE G A, NUMPRASANTHAI A, BUCKLEY A N. Bench-scale flotation of chrysocolla with n-octanohydroxamate [J]. Minerals Engineering, 2012, 36−38(5): 12−20.

[9] CHOI J, CHOI S Q, PARK K, HAN Y, KIM H. Flotation behaviour of malachite in mono- and di-valent salt solutions using sodium oleate as a collector [J]. International Journal of Mineral Processing, 2016, 146: 38−45.

[10] DENG Tong, CHEN Jia-yong. Treatment of oxidised copper ores with emphasis on refractory ores [J]. Mineral Processing & Extractive Metallurgy Review, 1991, 7: 175−207.

[11] BARBARO M, URBINA R H, COZZA C. Flotation of oxidized minerals of copper using a new synthetic chelating reagent as collector [J]. International Journal of Mineral Processing, 1997, 50(4): 275−287.

[12] LI Fang-xu, ZHONG Hong, XU Hai-feng, JIA Hui, LIU Guang-yi. Flotation behavior and adsorption mechanism of α-hydroxyoctylphosphinic acid to malachite [J]. Minerals Engineering, 2015, 71(2): 188−193.

[13] FUERSTENAU D W, HERRERA-URBINA R, MCGLASHAN D W. Studies on the applicability of chelating agents as universal collectors for copper minerals [J]. International Journal of Mineral Processing, 2000, 58(1): 15−33.

[14] KIM G, PARK K, CHOI J. Bioflotation of malachite using different growth phases of Rhodococcus opacus: Effect of bacterial shape on detachment by shear flow [J]. International Journal of Mineral Processing, 2015, 143(6): 98−104.

[15] PARK K, PARK S, CHOI J, KIM G, TONG M. Influence of excess sulfide ions on the malachite-bubble interaction in the presence of thiol-collector [J]. Separation and Purification Technology, 2016, 168: 1−7.

[16] FENG Qi-cheng, ZHAO Wen-juan, WEN Shu-ming, CAO Qing-bo. Copper sulfide species formed on malachite surfaces in relation to flotation [J]. Journal of Industrial and Engineering Chemistry, 2017, 48: 125−132.

[17] GAO Zhi-yong, BAI Ding, SUN Wei, CAO Xue-feng, HU Yue-hua. Selective flotation of scheelite from calcite and fluorite using a collector mixture [J]. Minerals Engineering, 2015, 72: 23−26.

[18] JIN Jun-xun, GAO Hui-min, CHEN Xun-meng, PENG Yong-jun, MIN Fan-fei. The flotation of aluminosilicate polymorphic minerals with anionic and cationic collectors [J]. Minerals Engineering, 2016, 99: 123−132.

[19] VIDYADHAR A, KUMARI N, BHAGAT R P. Adsorption mechanism of mixed collector systems on hematite flotation [J]. Minerals Engineering, 2012, 26(1): 102−104.

[20] TIAN Jia, XU Long-hua, DENG Wei, JIANG Hao, GAO Zhi-yong. Adsorption mechanism of new mixed anionic/cationic collectors in a spodumene-feldspar flotation system [J]. Chemical Engineering

Science, 2017, 164: 99−107.
[21] MEHDILO A, ZAREI H, IRANNAJAD M, ARJMANDFAR H. Flotation of zinc oxide ores by cationic and mixed collectors [J]. Minerals Engineering, 2012, 36−38(10): 331−334.
[22] LEE J S, NAGARAJ D R, COE J E. Practical aspects of oxide copper recovery with alkyl hydroxamates [J]. Minerals Engineering, 1988, 11: 929−939.
[23] HANSON J S, FUERSTENAU D W. The electrochemical and flotation behavior of chalcocite and mixed oxide/sulfide ores [J]. International Journal of Mineral Processing, 1991, 33: 33−47.
[24] LOTTER N O, BRADSHAW D J. The formulation and use of mixed collectors in sulphide flotation [J]. Minerals Engineering, 2010, 23(11): 945−951.
[25] JANG Hao, XU Long-hua, HU Yue-hua, WANG Dian-zuo, LI Chang-kai, MENG Wei, WANG Xing-jie. Flotation and adsorption of quaternary ammonium cationic collectors on diaspore and kaolinite [J] Transactions of Nonferrous Metals Society of China, 2011, 21: 2528−2534.
[26] PARK K, PARK S, CHOI J, KIM G, TONG M. Influence of excess sulfide ions on the malachite-bubble interaction in the presence of thiol-collector [J]. Separation and Purification Technology, 2016, 168: 1−7.
[27] GAO Zhi-yong, SUN Wei, HU Yue-hua. New insights into the dodecylamine adsorption on scheelite and calcite: An adsorption model [J]. Minerals Engineering, 2015, 79(8): 54−61.
[28] ZHANG Ya-hui, CAO Zhao, CAO Yong-dan, SUN Chuan-yao. FTIR studies of xanthate adsorption on chalcopyrite, pentlandite and pyrite surfaces [J]. Journal of Molecular Structure, 2013, 1048: 434−440.
[29] LAI Guo-yin, GUO Feng-feng, ZHENG Yue-qin. Highly enantioselective Henry reactions in water catalyzed by a copper tertiary amine complex and applied in the synthesis of (S)-N-trans-feruloyl octopamine [J]. Chemistry, 2011, 17(4): 1114−1117.
[30] TEO L S, CHEN C Y, KUO J F. Fourier transform infrared spectroscopy study on effects of temperature on hydrogen bonding in amine-containing polyurethanes and poly(urethane−urea)s [J]. Macromolecules, 1997, 30(6): 1793−1799.

组合捕收剂硫化浮选氧化铜的机理和应用

印万忠[1,2]，孙乾予[1]，李 东[1]，唐 远[1]，付亚峰[1]，姚 金[1]

1. 东北大学 资源与土木工程学院，沈阳 110819；
2. 福州大学 紫金矿业学院，福州 350116

摘 要：通过浮选试验、芘荧光探针、zeta 电位和红外光谱分析，研究组合捕收剂丁钠黄药(NaBX)和十二胺(DDA)对氧化铜浮选的影响。单矿物浮选试验表明，在 pH 7~11 条件下，NaBX+DDA 的浮选效果优于 NaBX，其中 NaBX 与 DDA 的最佳摩尔比为 2:1。实际矿的浮选试验表明，NaBX 和 DDA 的用量为(100+54) g/t 时，精矿中铜的品位和回收率分别为 15.93%和 76.73%。芘荧光探针结果表明，NaBX+DDA 可降低胶束在矿浆中形成的浓度。Zeta 电位和红外光谱测试结果表明，NaBX+DDA 通过化学吸附、氢键吸附和静电吸附作用在孔雀石表面，并生成黄原酸铜和铜胺络合物。

关键词：氧化铜；组合捕收剂；浮选；吸附；红外光谱

(Edited by Xiang-qun LI)